Fingerprinting of Galectins in Normal, *P. aeruginosa*–Infected, and Chemically Burned Mouse Corneas

Wei-Sheng Chen,[1] Zhiyi Cao,[2] Laetitia Truong,[3] Satoshi Sugaya,[2] and Noorjahan Panjwani[1,2,4]

[1]Program in Cell, Molecular & Developmental Biology, Sackler School of Graduate Biomedical Sciences, Tufts University, Boston, Massachusetts, United States
[2]New England Eye Center/Department of Ophthalmology, Tufts University, Boston, Massachusetts, United States
[3]Public Health and Professional Degree Programs, Tufts University School of Medicine, Boston, Massachusetts, United States
[4]Department of Developmental, Molecular and Chemical Biology, Tufts University, Boston, Massachusetts, United States

Correspondence: Noorjahan Panjwani, Department of Ophthalmology Tufts University School of Medicine, 136 Harrison Avenue, Boston, MA 02111, USA; noorjahan.panjwani@tufts.edu.

W-SC, ZC, and LT contributed equally to the work presented here and should therefore be regarded as equivalent authors.

Submitted: July 29, 2014
Accepted: December 15, 2014

Citation: Chen W-S, Cao Z, Truong L, Sugaya S, Panjwani N. Fingerprinting of galectins in normal, *P. aeruginosa*-infected and chemically burned mouse corneas. *Invest Ophthalmol Vis Sci*. 2015;56:515–525. DOI:10.1167/iovs.14-15338

Purpose. In this study, we aimed to assess whether the expression pattern of galectins is altered in *Pseudomonas aeruginosa*–infected and chemically burned mouse corneas.

Methods. Galectin (Gal) fingerprinting of normal, *P. aeruginosa*–infected, and silver nitrate–cauterized corneas was performed by Western blotting, immunofluorescence staining, and qRT-PCR.

Results. In normal corneas, Gal-1 was distributed mainly in the stroma, Gal-3 was localized mainly in epithelium, and Gal-7, -8, and -9 were detected in both corneal epithelium and stroma. Expression levels of the five galectins were drastically altered under pathological conditions. In both infected and cauterized corneas, overall Gal-3 expression was downregulated, whereas overall Gal-8 and -9 were upregulated. Changes in the expression level of Gal-7, -8, and -9 were distinct in the epithelium of infected and cauterized corneas. Expression of these three galectins was upregulated in corneal epithelium of infected corneas but not in cauterized corneas. Consistent with the changes in protein expression: (1) Gal-7, -8, and -9 mRNA expression was upregulated in cauterized corneas, and (2) Gal-3 mRNA was downregulated and Gal-9 mRNA expression was upregulated in infected corneas.

Conclusions. Our data demonstrate differential regulation of various members of the galectin family in the course of corneal infection and neovascularization. The emerging functionality of the sugar code of cell surface receptors via endogenous galectins reflect to the pertinent roles of the five tested galectins in the diseases of cornea.

Keywords: galectin, *Pseudomonas aeruginosa*, angiogenesis, cornea

Galectins (Gal) are a family of animal lectins that bind β-galactosides.[1,2] Galectins are present both inside and outside cells and function both intracellularly and extracellularly.[3,4] Functions of galectins include, but are not limited to, immune regulation, host-pathogen interactions, angiogenesis, re-epithelialization of wounds, and fibrosis. Galectins are expressed in the cells of the innate and adaptive immune system[5] and can have anti- or proinflammatory roles depending on the stage of infection and the degree of inflammation.[6,7] Galectins can also function as pattern-recognition receptors either to facilitate or to inhibit attachment/invasion of pathogens, such as virus, bacteria, protista, and fungi.[5,8] More recently, galectins have been shown to modulate angiogenic responses. Gal-1, -3, and -8 are proangiogenic[9–11] while Gal-9 is antiangiogenic.[12] Studies aimed at characterization of the role of galectins in wound healing have shown that several members of galectin family, including Gal-2, -3, -4, and -7, promote re-epithelialization of wounds.[13] In addition, it has been demonstrated that experimentally induced fibrosis is dependent on Gal-3 in a variety of tissues including lung, heart, and liver. Specifically, in the context of cornea, Gal-3 has been shown to play a key role in maintaining ocular surface barrier function through carbohydrate-dependent interactions with cell surface mucins.[14] It has also been demonstrated that Gal-3 and -7, but not Gal-1, promote corneal epithelial cell migration and re-epithelialization of corneal wounds.[15] Studies from our laboratory have also shown that corneal neovascularization is much reduced in Gal-3 knockout mice and that Gal-3 modulates VEGF-mediated angiogenesis by binding via its carbohydrate recognition domain (CRD) to N-glycans of VEGFR-2 and αvβ3 integrin, and subsequently activating the signaling pathways that promote the growth of new blood vessels.[10]

Gal-3 of corneal epithelial cells binds to lipopolysaccharide (LPS) of *Pseudomonas aeruginosa* to facilitate *P. aeruginosa* adhesion.[16] In addition, exogenous application of Gal-1 has been shown to suppress both *P. aeruginosa*– and herpes simplex virus (HSV)-induced corneal immunopathology by shifting the balance between effector T cells and regulatory T cells.[17,18] Both Gal-1 and -9 are thought to contribute to the immunosuppressive intraocular microenvironment and underlying immune privilege of the eye. Despite intensified interest in the functions of galectins, the galectin expression signature has thus far not been assessed in the context of the normal and diseased corneas. In an effort to fill this gap, the current study was designed to delineate the galectin expression pattern of normal, *P. aeruginosa*–infected, and chemically cauterized corneas.

Methods

Selection of Galectins

Although it is generally stated there are 15 members of galectin family, the actual number of authentic members of galectin family in mammalian tissues is smaller. Gal-5 has been found only in rat and is almost identical to the C-terminal CRD of rat Gal-9.[19,20] Gal-6 is only found in mouse and is almost identical to mouse Gal-4.[21] Gal-10 and -12 have relatively weak affinity for galactose-containing sugars. In fact, Gal-10 prefers mannose.[22–24] The name Gal-11 has been given to a galectin-related interfiber protein (GRIFIN), which is found in the lens. It too does not have carbohydrate-binding activity.[25] Interestingly, galectin nomenclature has omitted no. 13 and Gal-14 and -15 are found only in ovine and goat. Thus, for the analysis galectin signature relevant to human tissues, one should include Gal-1 to 4, and 7 to 9. However, Gal-2 and -4 are either not present or present only in trace amounts in normal or diseased corneas (Cao and Panjwani, unpublished). Therefore, of relevance to the cornea are Gal-1, -3, -7, -8, and -9. In this study, we assessed the expression pattern of these five galectins in normal, infected, and chemically burned eyes.

P. aeruginosa Infection

A *P. aeruginosa* cytotoxic strain 6077 was used to infect the right eyes of wild-type C57BL/6 mice (Jackson Laboratory, Bar Harbor, ME, USA). All animal procedures were approved by the Institutional Animal Care and Use Committee and were conducted in compliance with the ARVO Statements for the Use of Animals in Ophthalmic and Visual Research. Central corneas of anesthetized mice were scarified with three parallel 1-mm incisions using a 26-G needle, and a 5-μl drop of bacterial suspension (1 to 2×10^6 colony forming units) was applied to the eye. Corneas were harvested on days 2 and 8 post inoculation for Western blot analysis, immunofluorescence staining, or qRT-PCR. Three or more corneas were pooled and considered one biological replica. At least three biological replicas were used for each condition.

Silver Nitrate Cautery

Mice were anesthetized and a silver nitrate applicator (end diameter of 2.5 mm, coated with 75% silver nitrate and 25% potassium nitrate; Grafco, Memphis, TN, USA) was applied on the central cornea of the right eye of each animal for 5 seconds under a surgical microscope. The area of acute chemical burn was 4.89 mm^2. The corneas were rinsed with PBS, and ophthalmic antibiotic ointment (Alcon, Fort Worth, TX, USA) was topically applied to the operated eyes to prevent infection. Corneas were harvested on day 7 postsurgery for Western blot analysis, immunofluorescence staining, or qRT-PCR.

Corneal Whole-Mount Immunofluorescence Staining

The enucleated mouse eyes were fixed with 4% paraformaldehyde/PBS for 30 minutes at 4°C. The corneas were excised under a stereoscopic microscope and three to four radial cuts were made in the cornea by a blade. After washing with PBS three times (5 minutes each time), the corneas were fixed with iced methanol for 20 minutes at 25°C, washed again with PBS once and 0.3% Triton X-100/PBS twice, and placed individually in wells of a U-shaped 96-well plate and blocked with 5% BSA/0.3% Triton X-100/PBS for 30 minutes at 25°C. To quantitate the extent of angiogenesis, corneas were incubated overnight at 4°C with an Alexa Fluor 488-conjugated anti-mouse CD31 antibody (clone MEC13.3; 1:100 dilution; BioLegend, San Diego, CA, USA) in 5% BSA/0.3% Triton X-100/PBS. Tissues were washed with 0.3% Triton X-100/PBS three times, flattened, and mounted with a VECTASHIELD mounting medium (Vector Laboratories, Burlingame, CA, USA), and evaluated by the EVOS FL cell imaging system (Invitrogen, Waltham, MA, USA) using a ×2 objective. The $CD31^+$ blood vessel area of each cornea was quantified by ImageJ software (http://imagej.nih.gov/ij/; provided in the public domain by the National Institutes of Health, Bethesda, MD, USA) and presented as a percentage of the total corneal area outlined by the border of the outermost vessel of the limbal arcade.

Western Blot Analysis

Protein extracts of normal, infected, and chemically burned corneas were prepared in a radioimmunoprecipitation (RIPA) buffer supplemented with a protease inhibitor cocktail (cOmplete tablets; Roche Applied Science, Mannheim, Germany) and 2% SDS. Tissue lysates of whole corneas as well as isolated corneal epithelium and stroma were prepared. To separate epithelial sheets from the underlying stroma, corneas were incubated with 20 mM EDTA in Ca^{2+} and Mg^{2+}-free PBS (37°C, 20 minutes), and epithelial sheets were removed with forceps under a dissecting microscope. Since the center of *P. aeruginosa*–infected and $AgNO_3$-cauterized corneas had little epithelium, only the peripheral epithelial sheets were collected for analyses. For preparation of tissue lysates, whole corneas, epithelial sheets, and denuded stromal tissues from three to four corneas were pooled and considered one biological replica. Aliquots of lysates containing 30 μg of proteins were subjected to electrophoresis in 4% to 15% SDS-PAGE gels (Bio-Rad, Hercules, CA, USA). Protein blots of the gels were blocked with Odyssey blocking buffer (OBB; Li-Cor Biosciences, Lincoln, NE, USA) and incubated with goat anti-Gal-1 (1:1000; R&D Systems, Minneapolis, MN, USA) and rabbit anti-Gal-8 (1:750; Novus Biologicals, Littleton, CO, USA) primary antibodies in OBB (4°C, overnight). The secondary antibodies used were anti-goat IgG IRDye 800CW and anti-rabbit IgG IRDye 680LT (Li-Cor) diluted in OBB (1:10,000, 25°C, 45 minutes). Blots were then scanned with the Odyssey Infrared Imaging System using Image Studio v2.0 software (Li-Cor). After image acquisition, the blots were stripped using the NewBlot nitrocellulose stripping buffer (Li-Cor) and reprobed using rabbit anti-Gal-7 (1:10,000; Bethyl Lab, Montgomery, TX, USA) and rat anti-Gal-9 (clone 108A2, 1:1,000; BioLegend) antibodies overnight at 4°C. The secondary antibodies used were anti-rat IgG IRDye 800CW and anti-rabbit IgG IRDye 680LT (Li-Cor). After image acquisition, the blots were stripped again and reprobed with rat anti–Gal-3 (mAb M3/38; 1:5000) and mouse anti-β-actin (clone AC-15, 1:10,000; Santa Cruz Biotechnology, Dallas, TX, USA) as primary antibodies, and anti-rat IgG IRDye 800CW (Li-Cor) and anti-mouse IgG IRDye 680LT (Li-Cor) as secondary antibodies. Relative band intensity was quantified by Image Studio v2.0 software (Li-Cor). For total corneal extracts, data were normalized to β-actin expression. However, when corneal epithelium and stromal tissue were analyzed separately, as expected due to low-cell density, β-actin signal was relatively weak in the extracts of normal corneal stroma, which confounded accurate quantification of data based on actin normalization. Therefore, for isolated corneal epithelium and stromal tissues, quantification was based on the intensities without normalization to β-actin.

Immunofluorescence Staining

For immunofluorescence staining, frozen sections of the eyes were fixed with iced acetone (10 minutes, 25°C), blocked

Investigative Ophthalmology & Visual Science

with Image-iT FX signal enhancer (30 minutes, 25°C; Invitrogen), and immunostained using primary antibodies (1:100 dilution; same sources of the antibodies were used as indicated in the Western blot section) and Alexa Fluor 488-conjugated anti-rat, Alexa Fluor 568-conjugated anti-rabbit, or Alexa Fluor 488-conjugated anti-goat secondary antibodies (1:300 dilution in 5% BSA/PBS, 1 hour, 25°C; Invitrogen). Negative controls with no applied primary antibody were also used. Fluorescence images were acquired by Lieca TCS SPE imaging system (Leica, Buffalo Grove, IL, USA).

Quantitative RT-PCR

Total RNA was extracted from normal, infected and chemically burned mouse corneas using the RNeasy Mini Kit (Qiagen, Valencia, CA, USA). At least four corneas were pooled and considered one biological replica. Four biological replicas ($N = 4$) were used. The quality and yield of each RNA preparation was determined using the Agilent BioAnalyzer 2100 with RNA Pico Lab-Chips (Agilent, Santa Clara, CA, USA). Quantitative RT-PCR was performed using Mx3000P or Mx4000 thermal cyclers (Stratagene, Santa Clara, CA, USA). Complementary DNA was synthesized from 100 ng total RNA using the High-Capacity cDNA Reverse Transcriptase Kit (Invitrogen). Polymerase chain reaction amplification was performed in triplicate using gene-specific primers for β-actin, Gal-1, -3, -7, -8, and -9 (Invitrogen) and a master mix (Taqman Gene Expression Master Mix; Invitrogen). Assay IDs for β-actin, Gal-1, -2, -3, -4, -7, -8, and -9 are Mm 00607939, Mm00839408, Mm00840285, Mm00802901, Mm01179060, Mm00456135, Mm01332239, and Mm00495295, respectively. For amplification, after an initial denaturation step (95°C for 10 minutes), the reactions were subjected to 40 cycles involving denaturation (95°C for 15 seconds), and annealing plus extension (60°C for 1 minute). A threshold cycle value (C_t) was calculated from each amplification plot. Quantification data of each gene were normalized to the expression of β-actin. Relative gene expression was calculated with the ΔΔCT method. A value of 1.0 was given to the expression of each gene in the control cornea and the expression values for all other samples were calculated as a change in expression level with respect to the control cornea.

Results

Animal Models

The two mouse models used in the current study represent two different categories of inflammation: pathogen-induced inflammation and sterile inflammation, which is elicited by self-danger/damage signals. As expected, significant opacity was detected in the corneas of both infected and cauterized eyes (Fig. 1A). In infected eyes, blood vessels were seen, particularly in the limbal area, in the corneas of day 8 post-infection (pi) group ($N = 32$) but not in the corneas of day 2 pi group ($N = 27$). To visualize blood vessels in cauterized (day 7, $N = 27$) and infected eyes (day 8 pi), corneal flat mounts were stained with anti-CD31 antibody and the neovascularized areas were quantified. The extent of corneal neovascularization was similar in the cauterized and the infected eyes (Fig. 1B).

Expression Pattern of Galectins in *P. aeruginosa*–Infected Corneas

To determine the galectin expression levels in normal and infected corneas, tissue lysates of whole corneas collected on days 2 and 8 pi (30 μg) were subjected to electrophoresis. Protein blots were probed with specific antibodies for β-actin and Gal-1, -3, -7, -8, and -9. Fold-change values relative to β-actin expression of various galectins on days 2 and 8 pi are shown in Figure 2. Expression level of Gal-1, -3, and -7 were significantly decreased compared with normal mouse corneas on days 2 (percent reduction: Gal-1 and -3: 70%; Gal-7: 35%) and 8 pi (percent reduction: Gal-1: 37%; Gal3: 55%; Gal-7: 32%). In contrast, expression of Gal-8 and -9 was upregulated compared to normal mouse corneas on day 2 (percent increase: Gal-8: 21%; Gal-9: 78%) and day 8 pi (percent increase: Gal-8: 270%; Gal-9: 420%). Prior to use, each antibody was tested for specificity against recombinant human Gal-1, -3, -7, and -8 by Western blot analysis. Antibodies against Gal-1, -3, -7, and -8 did not cross-react with any other human galectins tested. The anti-mouse Gal-9 antibody does not cross-react to human Gal-9,[26–28] so the specificity of the antibody was not tested.

Immunofluorescence Localization of Galectins in Control and Infected Corneas

To investigate galectin expression pattern at the tissue level, frozen sections of normal and infected corneas were immunostained with antigalectin antibodies. In normal corneas, Gal-1 immunoreactivity was mainly detected in corneal stroma, immunoreactivity of Gal-3 was detected mainly in corneal epithelium (Fig. 3), and immunoreactivity of Gal-7, -8, and -9 was detected in both epithelium and stroma (Fig. 3). In *P. aeruginosa*-infected corneas, immunoreactivity of Gal-3, -7, -8, and -9 was detected in stroma as well as epithelium, whereas Gal-1 immunoreactivity was detected mainly in corneal stroma (Fig. 3, Table). No staining was detected in control tissue sections incubated with secondary antibodies alone (Fig. 3).

Analysis of Galectin Expression in Epithelium and Stroma of Normal and Infected Corneas by Western Blot

To further analyze the galectin expression in different layers of corneas, corneal epithelium and stroma were separated by incubation in 20 mM EDTA for 20 minutes. Protein lysates (30 μg) from corneal epithelium and stroma collected on day 8 pi were subjected to electrophoresis. Protein blots were probed with specific antibodies for β-actin and Gal-1, -3, -7, -8, and -9. On day 8 pi, Gal-3 expression was markedly downregulated (percent reduction: 58%), whereas Gal-1, -7, -8, and -9 were upregulated in epithelium of infected corneas compared with that of control corneas (fold increase: Gal-1: 10-fold; Gal-7: 2.6-fold; Gal-8: 1.6-fold; Gal-9: 2.6-fold; Fig. 4Bi). In contrast, all five galectins were upregulated in the stroma of the infected corneas (fold increase: Gal-1: 1.8-fold; Gal-3: 1.3-fold; Gal-7: 2.9-fold; Gal-8: 3.0-fold; Gal-9: 6.4-fold; Fig. 4Bii). Of note, although, in the immunofluorescence staining, Gal-1 was not detected in epithelium on day 8 pi (Fig. 3), Western blot analysis revealed that the lectin is upregulated in the epithelium of day 8 pi corneas. We reason that, in the immunofluorescence staining study, the robust immunoreactivity of Gal-1 in corneal stroma outshines the immunoreactivity of Gal-1 in corneal epithelium.

Galectin mRNA Expression Pattern in Control and *P. aeruginosa*–Infected Corneas

As determined by qRT-PCR, mRNA expression levels of galectins mRNA were ranked as Gal-3 > Gal-7 > Gal-8 > Gal-1 > Gal-9 in normal corneas; Gal-3 > Gal-7 > Gal-1 > Gal-8 >

Investigative Ophthalmology & Visual Science

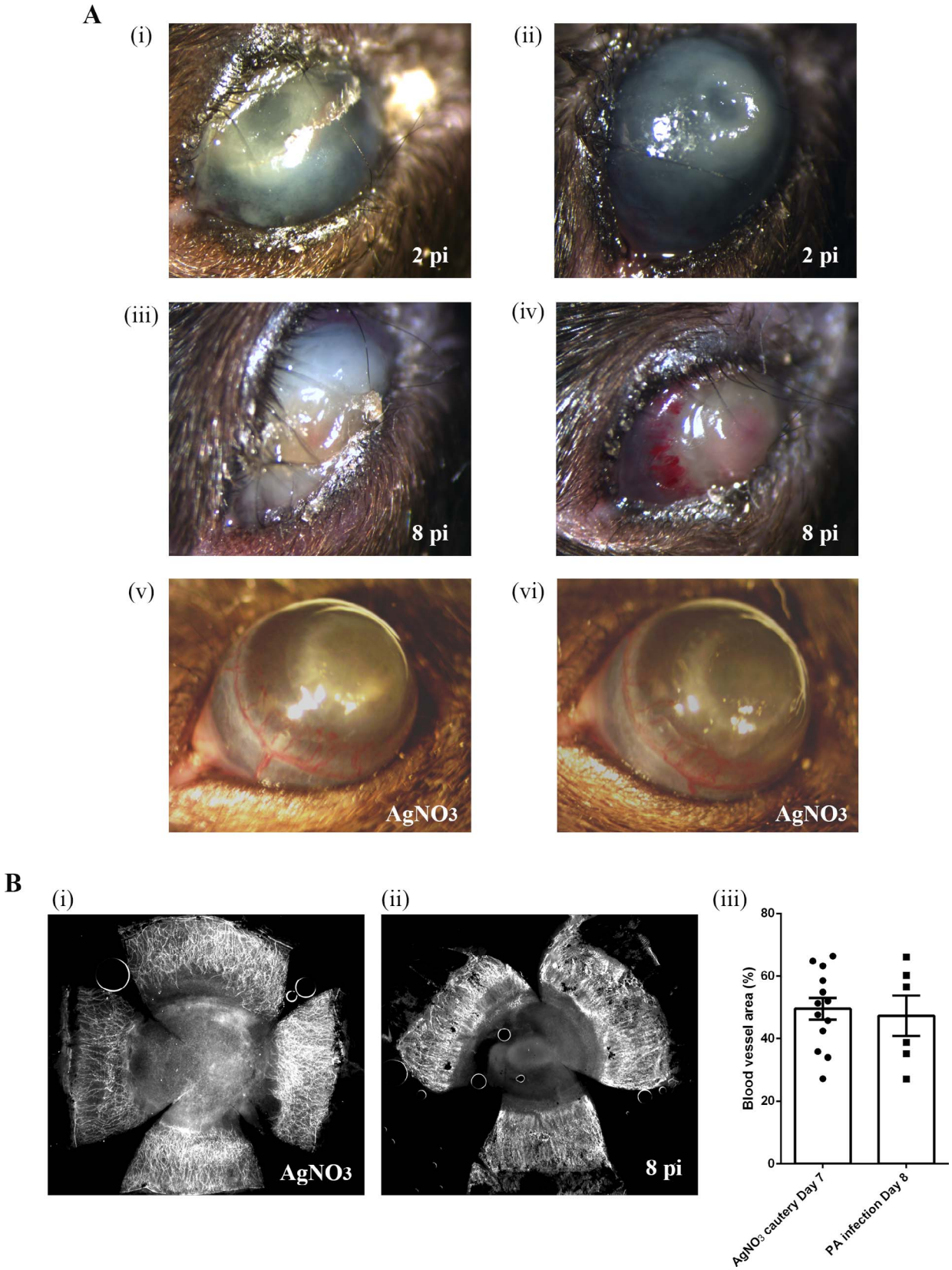

Figure 1. Photomicrographs of infected and cauterized mouse eyes. (**A**) Corneas of C57BL/6 mice were infected with *P. aeruginosa* or cauterized by treatment with $AgNO_3$. Photomicrographs shown are representative of infected corneas collected on day 2 pi (i, ii; $N = 27$) and day 8 pi (iii, iv; $N = 32$), and cauterized corneas collected on day 7 (v, vi; $N = 27$). (**Bi**, ii) Representative immunofluorescence images of $AgNO_3$-cauterized (day 7 post cauterization) and infected (day 8 pi) corneas stained with anti-CD31. Blood vasculatures were quantified as described in the Methods.

Investigative Ophthalmology & Visual Science

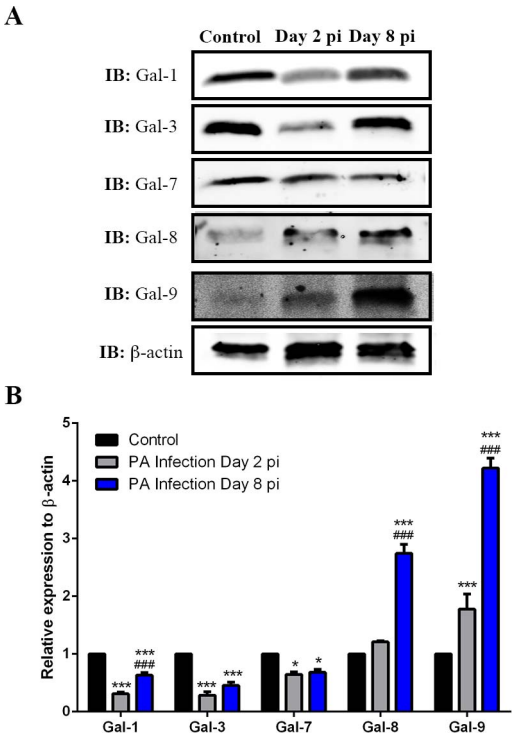

FIGURE 2. Detection of galectins in normal and infected corneas by Western blotting. Lysates of whole corneas containing 30 μg of protein were subjected to electrophoresis in 4% to 15% SDS-PAGE gels. Protein blots of the gels were probed using antibodies as descried in Methods. (**A**) Representative immunoblots. (**B**) Relative band intensity was quantified by ImageStudio. Expression value of each galectin was normalized to β-actin, a value of 1.0 was given to the expression of each galectin in the normal cornea and the expression values of galectins in the infected corneas were calculated as fold changes with respect to the control cornea. Three to four corneas were pooled and considered one biological replica. $N = 4$. Data are plotted as mean ± SEM and analyzed using one-way ANOVA. $^{*}P < 0.05$, $^{**}P < 0.01$, $^{***}P < 0.001$ versus control. $^{\#\#\#}P < 0.001$ versus day 2 pi.

Gal-9 on day 2 pi corneas; and Gal-3 > Gal-1 > Gal-7 > Gal-8 > Gal-9 in day 8 pi corneas. Fold changes relative to β-actin expression of various galectins on days 2 and 8 pi is shown in Figure 5. Statistically significant differences were observed in relative gene expression levels of various galectins between normal and infected corneas on days 2 and 8 pi. Gal-1 mRNA expression levels increased 10-fold by days 2 and 8 pi, while Gal-3 and Gal-8 showed a 50% decrease by day 2 pi and a 75% decrease by day 8 in the infected corneas compared with the control cornea. Gal-7 mRNA expression increased by 2-fold on day 2 pi but restored to normal levels by day 8 pi. Gal-9 mRNA expression increased at both time points by 2.5- and 1.5-fold, respectively. Thus, consistent with changes in protein expression, Gal-3 mRNA was downregulated and Gal-9 mRNA expression was upregulated in infected corneas (Figs. 2 and 5). However, changes in protein expression level of Gal-1, -7, and -8 did not reflect changes in corresponding mRNA expression level. For example, compared with normal corneas, infected corneas exhibited: (1) increased Gal-1 mRNA but reduced Gal-1 protein expression on both days 2 and 8 pi, (2) decreased Gal-7 protein expression, but increased Gal-7 mRNA expression on day 2 pi, and (3) increased Gal-8 protein expression but reduced Gal-8 mRNA on day 8 pi. These results were reproducible in four independent preparations of corneal protein extracts and mRNA.

Expression Pattern of Galectins in Chemically Burned Mouse Corneas: Western Blot Analysis

Analysis of the lysates of whole corneas revealed that compared with normal corneas, in chemically injured corneas, Gal-1 expression did not change, Gal-3 expression was significantly reduced (percent reduction: 60%) and the expression of Gal-7, -8, and -9 was significantly increased (fold increase: Gal-7: 8.2-fold; Gal-8: 11-fold; Gal-9: 5-fold; Fig. 6). Thus, in both infected and cauterized corneas, Gal-3 expression was downregulated, whereas Gal-8 and -9 were upregulated (Figs. 2 and 6). Changes in the expression level of Gal-1 and -7 were distinct in infected and cauterized corneas. Expression of these two galectins were downregulated in infected corneas but was either upregulated (Gal-7) or did not change (Gal-1) in cauterized corneas.

Immunofluorescence Localization of Galectins in Chemically Burned Corneas

Similar to infected corneas, robust immunoreactivity of all five galectins was detected in corneal stroma of the cauterized eyes (Fig. 7). Four different cauterized eyes were used and the immunofluorescence staining of all galectins tested in this study showed consistent results.

Analysis of Galectin Expression in Epithelium and Stroma of Normal and Chemically Burned Corneas by Western Blot

For this study, corneal epithelium and stroma of normal and cauterized (day 7) corneas were separated, lysed with lysis buffer, and subjected to Western blotting. Compared with control corneas, in epithelium of cauterized corneas, Gal-1 expression was upregulated (percent increase: Gal-1: 223%), whereas Gal-3 expression was markedly downregulated (percent reduction: 96%), and there was no change in Gal-7, -8, and -9 expression (Fig. 8Bi). In the stroma of cauterized corneas, expression of these five galectins was upregulated (fold increase: Gal-1: 1.9-fold; Gal-3: 3.0-fold; Gal-7: 5.1-fold; Gal-8: 2.4-fold; Gal-9: 1.4-fold; Fig. 8Bii).

Galectin mRNA Expression Pattern in Chemically Burned Mouse Corneas

As determined by qRT-PCR using RNA preparations of whole corneas, mRNA expression levels of galectins were ranked as Gal-3 > Gal-7 > Gal-8 > Gal-1 > Gal-9 in normal corneas and Gal-1 > Gal-7 > Gal-3 > Gal-8 > Gal-9 in cauterized corneas. Messenger RNA expression levels of Gal-1, -3, -7, -8, and -9 were all increased on day 7 post cauterization compared with normal mouse cornea (Fig. 9; fold increase: Gal-1: 41-fold; Gal-3: 1.85-fold; Gal-7: 34-fold; Gal-8: 1.82-fold; Gal-9: 16-fold). Thus, consistent with changes detected by Western blot analysis, Gal-7, -8, and -9 mRNA expression was upregulated in cauterized corneas. However, changes in the protein expression of Gal-1 and -3 did not reflect changes in corresponding mRNA expression level. Compared with normal corneas, cauterized corneas expressed decreased Gal-3 protein, but increased Gal-3 mRNA. While Gal-1 protein expression level was similar in both normal and cauterized corneas, Gal-1 mRNA expression was higher in cauterized corneas. The extent of change in the expression level of mRNA transcripts and the respective proteins may not be identical for a variety of reasons, such as variation in the RNA and protein turnover rates and stability as well as variations in the translational ratio

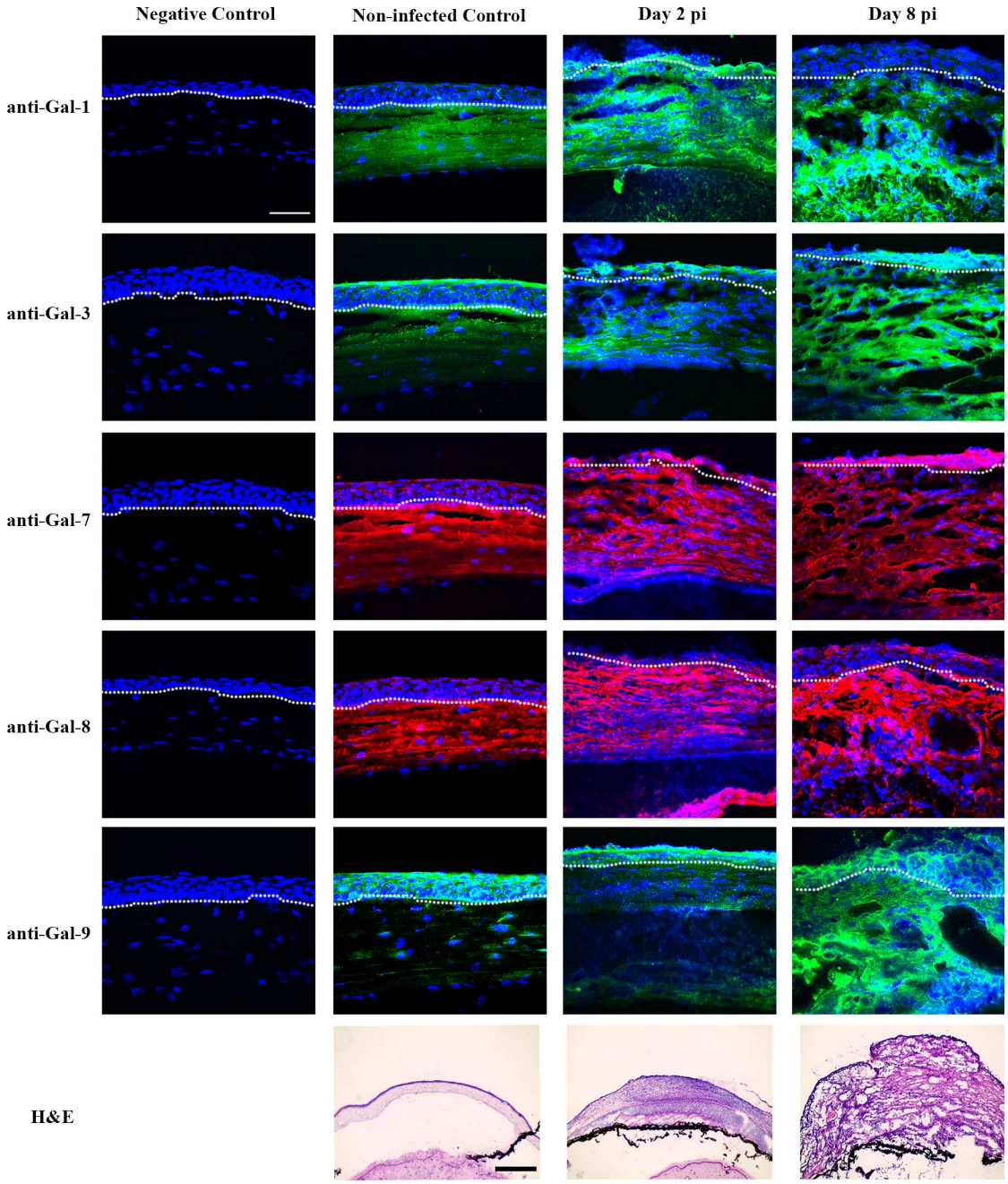

Figure 3. Immunofluorescence localization of galectins in normal and infected mouse corneas. Frozen tissue sections of normal and infected eyes were immunostained using antibodies against Gal-1, -3, -7, -8, and -9, and Alexa fluor 488-conjugated anti-goat (for Gal-1, *green*), Alexa fluor 488-conjugated anti-rat (for Gal-3 and -9, *green*) and Alexa fluor 568-conjugated anti-rabbit (for Gal-7 and Gal-8, *red*), followed by counterstaining with DAPI (*blue*). No immunoreactivity was detected in corneas, which were treated the same way as the experimental group except that the step involving incubation with the primary antibody was omitted (negative control). Tissue sections of the corneas stained with hematoxylin and eosin (H&E) are shown in the bottom panel. $N \geq 4$ for each galectin. *White dash lines* outline the border between corneal epithelium and stroma. Note that in normal corneas, Gal-1 is expressed mainly in corneal stroma, Gal-3 is expressed mainly in corneal epithelium, and Gal-7, -8, and -9 are present in both epithelium and stroma, and in *P. aeruginosa*–infected corneas, immunoreactivity of Gal-3, -7, -8 and -9 is detected in both corneal epithelium and stroma, whereas Gal-1 is localized mainly in corneal stroma. *Scale bar* in immunofluorescence images: 50 μm. *Scale bar* in H&E staining images: 100 μm.

of mRNA per protein among different cell types of the infiltrated infected and cauterized corneas.[29–34]

Discussion

We demonstrated here that Gal-1, -3, -7, -8, and -9, are expressed in normal mouse cornea, and under pathological conditions, expression levels and distribution of various galectins are drastically altered. In normal corneas, Gal-3 is mainly localized in epithelium, Gal-7, -8, and -9 are distributed in corneal epithelium and stroma, and Gal-1 is localized mainly in corneal stroma. All five galectins are highly upregulated in the insulted corneal stroma, whereas Gal-3 expression is markedly downregulated in insulted corneal epithelium.

Investigative Ophthalmology & Visual Science

Table. Galectin Staining Patterns of Normal, *P. aeruginosa*–Infected and Chemically Burned Mouse Corneas

	Normal		*P. aeruginosa*–Infected		Chemically Burned	
Galectin	**Epithelium**	**Stroma**	**Epithelium**	**Stroma**	**Epithelium**	**Stroma**
Gal-1	−	+	−/+*	++	−/+	++
Gal-3	++	−/+	+	++	+	++
Gal-7	+	+	+	++	+	++
Gal-8	+	+	+	++	+	++
Gal-9	+	−/+	+	++	+	++

−, negative; −/+, trace; +, moderate; ++, intense.

* No Gal-1 immunoreactivity was detected in the epithelium of 3/6 day 2 *P. aeruginosa*–infected corneas and 9/12 day 8 *P. aeruginosa*–infected corneas. In 3/6 day 2 infected corneas and in 3/12 day 8 infected corneas, positive Gal-1 immunoreactivity was detected in some regions of epithelium.

Source of galectins in the insulted corneal stroma can be infiltrating immune cells,[35] injured epithelium, activated tissue-resident macrophages, and endothelial cells of new blood vessels.

In our earlier study using paraffin-embedded tissue sections developed with diaminobenzidine, Gal-7 was detected mainly in corneal epithelium.[36] However, in the current study, both by Western blotting and immunofluorescence staining using frozen sections, Gal-7 was detected in both normal corneal stroma and epithelium. We have tested the specificity of the antibodies, and the anti-Gal-7 antibody that we used in this study has no cross-reactivity against Gal-1, -3, -8, and -9. In addition, no immunoreactivity was detected if the antibody was preincubated with recombinant Gal-7 prior to use (data not shown). Thus, we are able to place a high level of confidence in our observation that Gal-7 is expressed in corneal stroma, in addition to corneal epithelium. In this respect, it is known that Gal-7, which was originally considered a marker for epithelial cells, is also expressed in the mesenchymal stroma of the E11.5 undifferentiated genital ridge[37] and decidualized stroma of very late secretory phase endometria.[38] As for the source of Gal-7 we detected in the corneal stroma, it is possible that the lectin is secreted by corneal epithelial cells and deposited in the corneal stroma.

In this study, we used two different mouse models representing sterile and nonsterile inflammation. Antigen presenting cells recognize both pathogen-associated molecular patterns (PAMPs) from microbes (nonsterile inflammation, stranger model)[39] and damage-associated molecular patterns (DAMPs) from stressed, damaged and/or dying self-cells in the local tissue (sterile inflammation, danger model).[40] Both PAMPs and DAMPs induce inflammation by some shared receptors such as toll-like receptor 4 and receptor for advanced glycation end products (RAGE), as well as by distinct mechanisms. In this respect, a recent study has demonstrated that microRNA expression induced by DAMPs and PAMPs has a distinct signature; expression of miR-34c and miR-214 is increased in cells stimulated with DAMP, but not PAMP.[41] Galectins are considered DAMPs and receptors for PAMPs.[42]

We report here that changes in the expression levels of three of the five galectins tested (Gal-3, -8, and -9) were similar in both models. Overall, in both infected and cauterized corneas, Gal-3 expression was downregulated, whereas Gal-8 and -9 were upregulated. Changes in the expression level of Gal-1 and -7 were distinct in infected and cauterized corneas (Figs. 2 and 6). Overall expression of these two galectins was downregulated in infected corneas but was either upregulated (Gal-7) or did not change (Gal-1) in cauterized corneas. Regardless of whether whole corneas were analyzed or corneal epithelial and stromal layers were analyzed separately, Gal-8 and -9 were upregulated in both infected and cauterized corneas. Decrease in Gal-3 expression in infected and cauterized corneas was largely due to the reduced expression of this lectin in corneal epithelium. Intriguingly, when epithelial and stromal layers were analyzed separately, Gal-1 and -7 expression was upregulated in both corneal epithelium and stroma, whereas when whole corneas were analyzed the expression of both these lectins was downregulated. Such a discrepancy, however, is readily explicable. Since galectins are soluble proteins and distributed in the extracellular matrix, tissue fluid, cell membrane, and cytosol, it is possible that tissue fluid containing soluble galectins can leach out from inflamed corneas during incubation with EDTA and/or during separation of epithelial and stromal tissues. For Gal-1 and -7, the amounts of these two lectins in tissue fluid may be trace; therefore, the separation process of the tissue sheets may concentrate the two lectins.

Gal-1 has been shown to suppress both *P. aeruginosa*– and HSV-induced corneal immunopathology by shifting the balance between effector T cells and regulatory T cells, and to inhibit proinflammatory cytokine production from innate immune cells.[17,18,43,44] Gal-3 binds to the LPS of *P. aeruginosa* and may facilitate the invasion when the cornea gets infected.[16] Thus, in contrast to the protective effect of Gal-1 on immunopathology of Pseudomonas keratitis, it is possible that Gal-3 may exacerbate the infection. On the other hand, Gal-3 may also have protective effect due to its ability to accelerate re-epithelialization of corneal wounds.[15] Clearly, additional studies are needed to delineate the role of Gal-3 in the pathogenesis of Pseudomonas keratitis.

The role of Gal-7, -8, and -9 in *P. aeruginosa*–mediated corneal pathogenesis has thus far not been characterized. It has been reported that neutralizing Gal-9 abrogates the immune privilege status of the cornea and that local subconjunctival injections of Gal-9 diminishes the severity of HSV keratitis as well as the degree of corneal neovascularization in the mouse animal model.[45,46] Considering that Gal-9 deficiency aggravates several autoimmune diseases[46] and that exogenous Gal-9 increases effector T cell apoptosis and promotes regulatory T cell polarization,[47,48] it is possible that the upregulation of Gal-9 in the infected cornea may help dampen the corneal inflammation during *P. aeruginosa* infection.

As described above, changes in the expression level of Gal-7, -8, and -9 were distinct in the epithelium of infected and cauterized corneas. The expression level of the three galectins was upregulated in infected corneas, but did not change in cauterized corneas. The significance of this observation is not clear at this time. However, the three galectins in infected corneas may function as receptors for PAMPs and the upregulation may be related to the defense mechanism in corneal epithelium.

Angiogenesis is an important process during wound healing. Previous studies have shown that Gal-1, -3, -8, and -9 are involved in modulating angiogenesis. Gal-1 and -3 activate

Investigative Ophthalmology & Visual Science

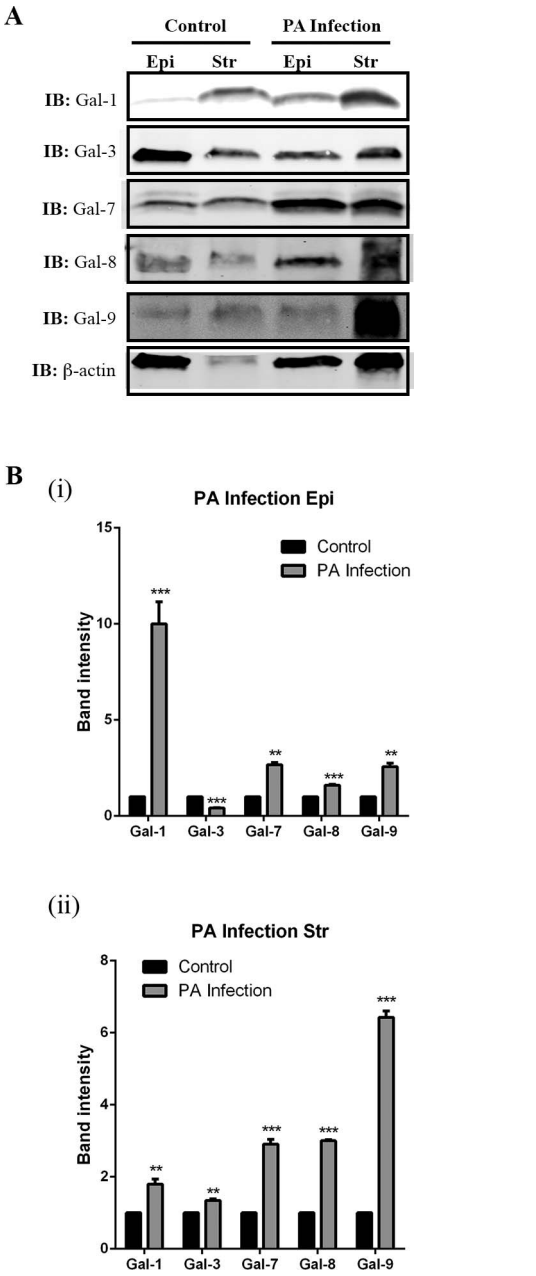

Figure 4. Galectin expression in corneal epithelium and stroma in normal and infected eyes on day 8 pi. Corneal epithelial and stromal sheets were separated by incubation in 20 mM EDTA for 20 minutes. Aliquots of the lysates containing 30 μg of protein were subjected to electrophoresis in 4% to 15% SDS-PAGE gels. Protein blots of the gels were probed using antibodies as descried in Methods. (**A**) Representative immunoblots. (**B**) Band intensity was quantified by ImageStudio. Although equal amounts of lysates were used, the intensity of β-actin in normal cornel stroma is less than other conditions. Therefore, the galectin expression is not normalized to β-actin. Instead, a value of 1.0 was given to the expression of each galectin in the normal cornea and the expression values of galectins in the infected corneas were calculated as fold changes with respect to the control cornea. Three to four corneas were pooled and considered one biological replica. $N = 3$. Data are plotted as mean ± SEM and analyzed using Student's *t*-test. $^{**}P < 0.01$, $^{***}P < 0.001$ versus control.

VEGFR-2,[10,49–51] Gal-8 promotes angiogenesis in a CD166-dependent manner,[11] and Gal-9 inhibits angiogenesis by an unknown mechanism.[12] In addition to their direct effect on endothelial cells, Gal-1, -3, and -8 also activate platelets to

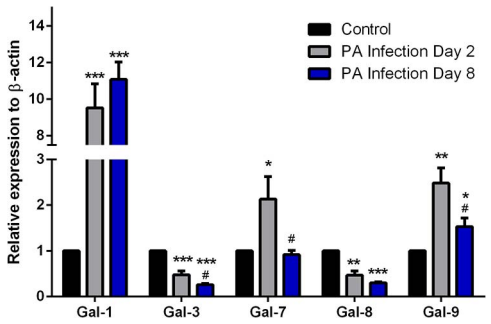

Figure 5. Analysis of mRNA expression levels of galectins in normal and infected corneas by qRT-PCR. Complementary DNA was synthesized from 100 ng each of total RNA preparations of normal and infected corneas using the High-Capacity cDNA Reverse Transcriptase Kit, and PCR amplification was performed in triplicate using gene-specific primers for β-actin, Gal-1, -3, -7, -8, and -9 and a Taqman master mix according to the manufacturer's instructions. A threshold cycle value (C_t) was calculated from each amplification plot. Quantification data of each gene were normalized to the expression of β-actin, a value of 1.0 was given to the expression of each gene in the control cornea and the expression values for galectins in infected corneas were calculated as a change in expression level with respect to the control cornea. At least four corneas were pooled and considered one biological replica. $N = 4$ for all galectins. Data are plotted as mean ± SEM and analyzed using one-way ANOVA. $^{*}P < 0.05$, $^{**}P < 0.01$, $^{***}P < 0.001$ versus control. $^{\#}P < 0.05$ versus day 2 pi.

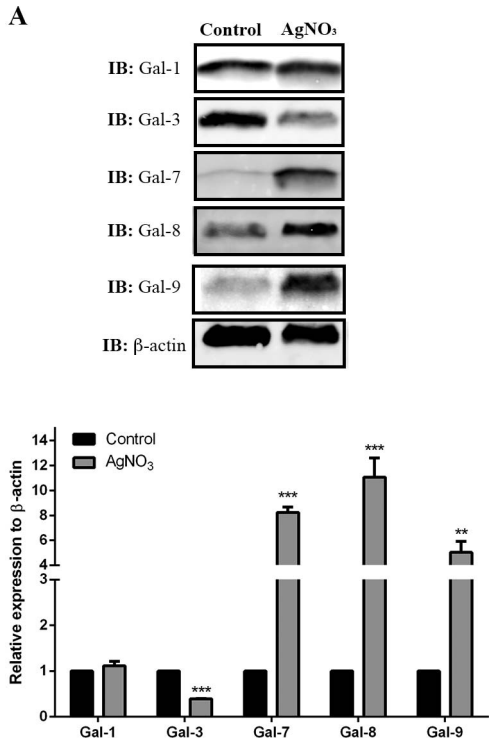

Figure 6. Detection of galectins in normal and cauterized corneas by Western blotting. (**A**) Lysates of whole corneas were used to assess Gal-1, -3, -7, -8, and, -9 protein expression on day 7 post cauterization by Western blot analysis as described in Methods. (**A**) Representative immunoblot. (**B**) Relative band intensity was quantified by ImageStudio. Expression value of each galectin was normalized to β-actin, a value of 1.0 was given to the expression of each galectin in the normal cornea and the expression values of galectins in the infected corneas were calculated as fold changes with respect to the control cornea. Three to four corneas were pooled and considered one biological replica. $N = 3$. Data are plotted as mean ± SEM of four independent experiments. $^{*}P < 0.05$, $^{**}P < 0.01$, $^{***}P < 0.001$ versus control.

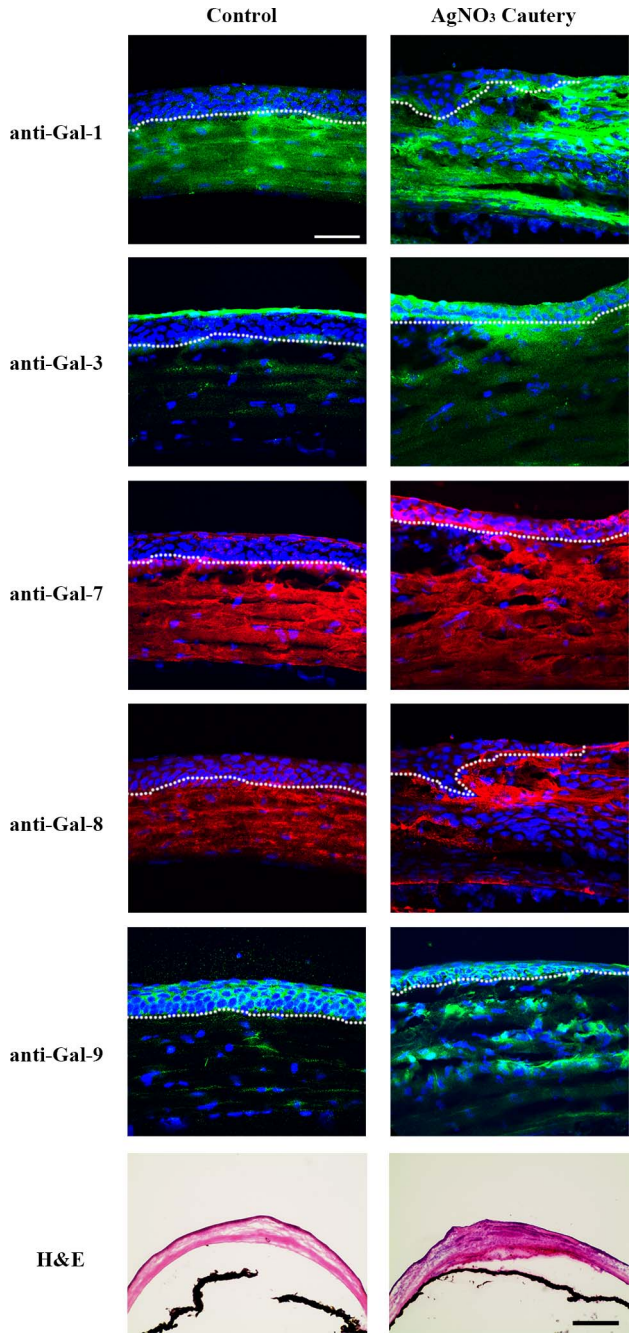

Figure 7. Immunofluorescence localization of galectins in normal and cauterized mouse corneas. Frozen sections of normal and cauterized corneas (day 7) were stained with antibodies against Gal-1, -3, -7, -8, and -9 as described in Figure 3 legend. Mouse corneas stained with H&E are shown in the bottom panel. Note that in cauterized corneas, Gal-1 is detected mainly in the stroma, whereas Gal-3, -7, -8, and -9 are detected in both corneal epithelium and stroma. $N \geq 4$ for each galectin. *Bar* in immunofluorescence images: 50 μm. *Bar* in H&E staining images: 100 μm.

release VEGF.[52] In this study, Western blot analysis revealed increased expression of Gal-3, -7, -8, and -9 in the corneal stroma, the site of neovascularization. As described earlier, Gal-3 promotes corneal neovascularization. The role of Gal-1, -7, -8, and -9 in corneal neovascularization has thus far not been investigated. Further investigations are required to determine the impact of the pro- and antiangiogenic galectins in the regulation of corneal neovascularization and to determine whether galectins can be targeted to inhibit pathological angiogenesis.

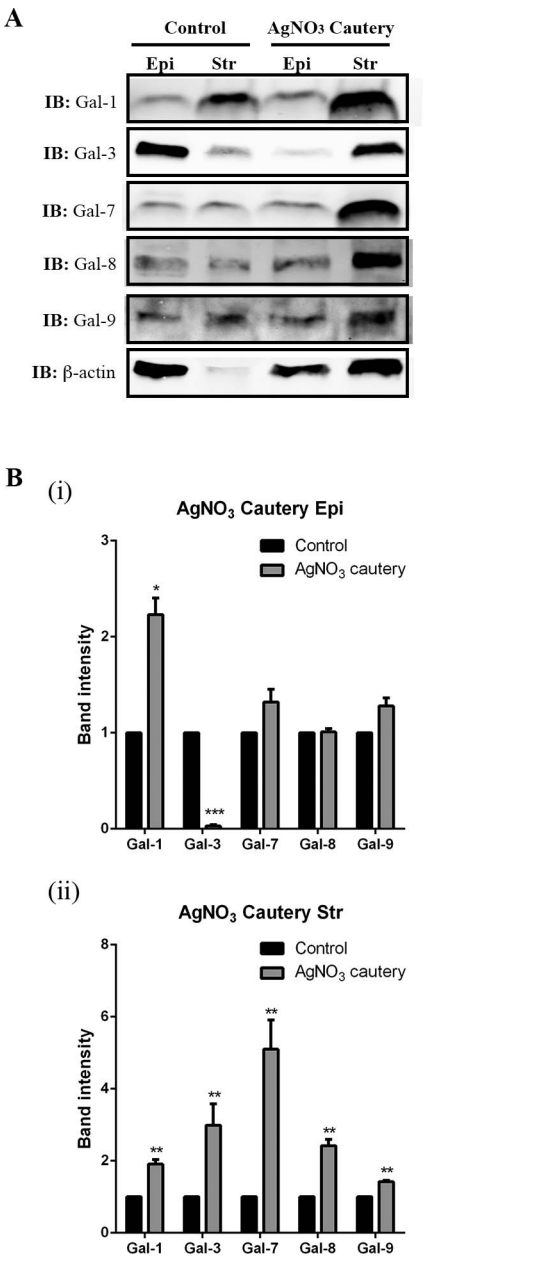

Figure 8. Galectin expression in corneal epithelium and stroma of normal and cauterized eyes on day 7 postcauterization. Corneal epithelial and stromal sheets were separated by incubation in 20 mM EDTA for 20 minutes. Aliquots of the lysates containing 30 μg of protein were subjected to electrophoresis in 4% to 15% SDS-PAGE gels. Protein blots of the gels were probed using antibodies as descried in Methods. (**A**) Representative immunoblots. (**B**) Band intensity was quantified by ImageStudio. A value of 1.0 was given to the expression of each galectin in the normal cornea and the expression values of galectins in the cauterized corneas were calculated as fold changes with respect to the control cornea. Three to four corneas were pooled and considered one biological replica. $N = 3$. Data are plotted as Mean ± SEM and analyzed using Student's *t*-test. $^{*}P < 0.05$, $^{**}P < 0.01$, $^{***}P < 0.001$ versus control.

Fibrosis is another cellular response during wound healing. The profibrotic role of Gal-3 has been established in heart, liver, lung, and kidney.[53–56] In this study, we found that Gal-3 was upregulated in the corneal stroma, the site of fibrosis, suggesting

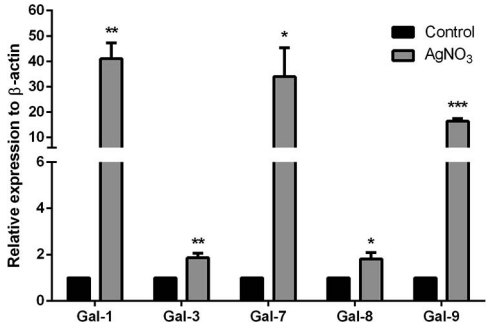

FIGURE 9. Analysis of mRNA expression levels of galectins in normal and cauterized corneas. Messenger RNA expression levels were analyzed for Gal-1, -3, -7, -8, and -9 by RT-qPCR on day 7 post cauterization as described in Figure 5 legend. At least four corneas were pooled and considered one biological replica. $N = 4$ for all galectins. Quantification data of each gene were normalized to the expression of β-actin. A value of 1.0 was given to the expression of each gene in the control cornea and the expression values for all other samples were calculated as a change in expression level with respect to the control cornea. Data are plotted as mean ± SEM and analyzed using Student's *t*-test. $^{*}P < 0.05$, $^{**}P < 0.01$, $^{***}P < 0.001$ versus control.

that Gal-3 may also play a role in promoting corneal fibrosis. In addition, Gal-1, -3, -7, and -8 have been shown to modulate the expression and/or function of matrix metalloproteinases,[57–62] which are involved in remodeling cellular matrix in the fibrotic microenvironment. Therefore, it is possible that Gal-1, -7, and -8 may also be involved in corneal fibrosis.

In conclusion, our study demonstrates the expression and differential regulation of various members of galectin family in the course of corneal infection and neovascularization. As described earlier, there is currently intense interest in characterizing the function of galectins because so many important cellular responses such as cell adhesion, migration, immune response, and angiogenesis are regulated by this class of lectins. It is our hope that this study will intensify investigations on characterizing the very important, but relatively underinvestigated, function of the sugar code of cell surface receptors via galectins in diseases of the eye.

Acknowledgments

The authors thank Thananya Thitiprasert for technical assistance and Dr. T. S. Zaidi for providing *P. aeruginosa* cytotoxic strain 6077.

Supported by National Eye Institute Grants R01EY007088, R01EY009349 (Bethesda, MD, USA), Massachusetts Lions Eye Research Fund (Boston, MA, USA), New England Corneal Transplant Fund (Boston, MA, USA), and an unrestricted award from Research to Prevent Blindness (New York, NY, USA).

Disclosure: **W.-S. Chen**, None; **Z. Cao**, None; **L. Truong**, None; **S. Sugaya**, None; **N. Panjwani**, None

References

1. Cooper DN. Galectinomics: finding themes in complexity. *Biochim Biophys Acta*. 2002;1572:209–231.
2. Liu FT, Rabinovich GA. Galectins as modulators of tumour progression. *Nat Rev Cancer*. 2005;5:29–41.
3. Liu FT, Patterson RJ, Wang JL. Intracellular functions of galectins. *Biochim Biophys Acta*. 2002;1572:263–273.
4. Hughes RC. Secretion of the galectin family of mammalian carbohydrate-binding proteins. *Biochim Biophys Acta*. 1999; 1473:172–185.
5. Vasta GR. Roles of galectins in infection. *Nat Rev Microbiol*. 2009;7:424–438.
6. Liu FT. Galectins: a new family of regulators of inflammation. *Clin Immunol*. 2000;97:79–88.
7. Rabinovich GA, Toscano MA. Turning 'sweet' on immunity: galectin-glycan interactions in immune tolerance and inflammation. *Nat Rev Immunol*. 2009;9:338–352.
8. Sato S, Ouellet M, St-Pierre C, Tremblay MJ. Glycans, galectins, and HIV-1 infection. *Ann N Y Acad Sci*. 2012;1253:133–148.
9. Thijssen VL, Postel R, Brandwijk RJ, et al. Galectin-1 is essential in tumor angiogenesis and is a target for antiangiogenesis therapy. *Proc Natl Acad Sci U S A*. 2006;103:15975–15980.
10. Markowska AI, Liu FT, Panjwani N. Galectin-3 is an important mediator of VEGF- and bFGF-mediated angiogenic response. *J Exp Med*. 2010;207:1981–1993.
11. Delgado VM, Nugnes LG, Colombo LL, et al. Modulation of endothelial cell migration and angiogenesis: a novel function for the "tandem-repeat" lectin galectin-8. *FASEB J*. 2011;25: 242–254.
12. Heusschen R, Schulkens IA, van Beijnum J, Griffioen AW, Thijssen VL. Endothelial LGALS9 splice variant expression in endothelial cell biology and angiogenesis. *Biochim Biophys Acta*. 2014;1842:284–292.
13. Cao Z, Saravanan C, Chen WS, Panjwani N. Examination of the role of galectins in cell migration and re-epithelialization of wounds. *Methods Mol Biol*. 2015;1207:317–326.
14. Argueso P, Guzman-Aranguez A, Mantelli F, Cao Z, Ricciuto J, Panjwani N. Association of cell surface mucins with galectin-3 contributes to the ocular surface epithelial barrier. *J Biol Chem*. 2009;284:23037–23045.
15. Cao Z, Said N, Amin S, et al. Galectins-3 and -7, but not galectin-1, play a role in re-epithelialization of wounds. *J Biol Chem*. 2002;277:42299–42305.
16. Gupta SK, Masinick S, Garrett M, Hazlett LD. Pseudomonas aeruginosa lipopolysaccharide binds galectin-3 and other human corneal epithelial proteins. *Infect Immun*. 1997;65: 2747–2753.
17. Suryawanshi A, Cao Z, Thitiprasert T, Zaidi TS, Panjwani N. Galectin-1-mediated suppression of Pseudomonas aeruginosa-induced corneal immunopathology. *J Immunol*. 2013;190: 6397–6409.
18. Rajasagi NK, Suryawanshi A, Sehrawat S, et al. Galectin-1 reduces the severity of herpes simplex virus-induced ocular immunopathological lesions. *J Immunol*. 2012;188:4631–4643.
19. Gitt MA, Wiser MF, Leffler H, et al. Sequence and mapping of galectin-5, a beta-galactoside-binding lectin, found in rat erythrocytes. *J Biol Chem*. 1995;270:5032–5038.
20. Wada J, Kanwar YS. Identification and characterization of galectin-9, a novel beta-galactoside-binding mammalian lectin. *J Biol Chem*. 1997;272:6078–6086.
21. Gitt MA, Colnot C, Poirier F, Nani KJ, Barondes SH, Leffler H. Galectin-4 and galectin-6 are two closely related lectins expressed in mouse gastrointestinal tract. *J Biol Chem*. 1998;273:2954–2960.
22. Leonidas DD, Elbert BL, Zhou Z, Leffler H, Ackerman SJ, Acharya KR. Crystal structure of human Charcot-Leyden crystal protein, an eosinophil lysophospholipase, identifies it as a new member of the carbohydrate-binding family of galectins. *Structure*. 1995;3:1379–1393.
23. Dyer KD, Rosenberg HF. Eosinophil Charcot-Leyden crystal protein binds to beta-galactoside sugars. *Life Sci*. 1996;58: 2073–2082.
24. Dyer KD, Handen JS, Rosenberg HF. The genomic structure of the human Charcot-Leyden crystal protein gene is analogous to those of the galectin genes. *Genomics*. 1997;40:217–221.
25. Ogden AT, Nunes I, Ko K, et al. GRIFIN, a novel lens-specific protein related to the galectin family. *J Biol Chem*. 1998;273: 28889–28896.
26. Tsuboi Y, Abe H, Nakagawa R, et al. Galectin-9 protects mice from the Shwartzman reaction by attracting prostaglandin E2-

producing polymorphonuclear leukocytes. *Clin Immunol*. 2007;124:221–233.

27. Sehrawat S, Reddy PB, Rajasagi N, Suryawanshi A, Hirashima M, Rouse BT. Galectin-9/TIM-3 interaction regulates virus-specific primary and memory CD8 T cell response. *PLoS Pathog*. 2010;6:e1000882.
28. Oomizu S, Arikawa T, Niki T, et al. Cell surface galectin-9 expressing Th cells regulate Th17 and Foxp3+ Treg development by galectin-9 secretion. *PloS One*. 2012;7:e48574.
29. Fontenot JD, Gavin MA, Rudensky AY. Foxp3 programs the development and function of CD4+CD25+ regulatory T cells. *Nat Immunol*. 2003;4:330–336.
30. Levy AP, Levy NS, Goldberg MA. Post-transcriptional regulation of vascular endothelial growth factor by hypoxia. *J Biol Chem*. 1996;271:2746–2753.
31. Czyzyk-Krzeska MF, Dominski Z, Kole R, Millhorn DE. Hypoxia stimulates binding of a cytoplasmic protein to a pyrimidine-rich sequence in the 3′-untranslated region of rat tyrosine hydroxylase mRNA. *J Biol Chem*. 1994;269:9940–9945.
32. McGary EC, Rondon IJ, Beckman BS. Post-transcriptional regulation of erythropoietin mRNA stability by erythropoietin mRNA-binding protein. *J Biol Chem*. 1997;272:8628–8634.
33. Shih SC, Claffey KP. Hypoxia-mediated regulation of gene expression in mammalian cells. *Int J Exp Pathol*. 1998;79:347–357.
34. Chiariotti L, Salvatore P, Frunzio R, Bruni CB. Galectin genes: regulation of expression. *Glycoconj J*. 2004;19:441–449.
35. Liu FT, Rabinovich GA. Galectins: regulators of acute and chronic inflammation. *Ann N YAcad Sci*. 2010;1183:158–182.
36. Cao Z, Said N, Wu HK, Kuwabara I, Liu FT, Panjwani N. Galectin-7 as a potential mediator of corneal epithelial cell migration. *Arch Ophthalmol*. 2003;121:82–86.
37. Timmons PM, Colnot C, Cail I, Poirier F, Magnaldo T. Expression of galectin-7 during epithelial development coincides with the onset of stratification. *Int J Dev Biol*. 1999;43:229–235.
38. Evans J, Yap J, Gamage T, Salamonsen L, Dimitriadis E, Menkhorst E. Galectin-7 is important for normal uterine repair following menstruation. *Mol Hum Reprod*. 2014;20:787–798.
39. Janeway CA Jr. Approaching the asymptote? Evolution and revolution in immunology. *Cold Spring Harb Symp Quant Biol*. 1989;54(Pt 1):1–13.
40. Matzinger P. Tolerance, danger, and the extended family. *Annu Rev Immunol*. 1994;12:991–1045.
41. Unlu S, Tang S, Wang E, et al. Damage associated molecular pattern molecule-induced microRNAs (DAMPmiRs) in human peripheral blood mononuclear cells. *PloS One*. 2012;7:e38899.
42. Sato S, St-Pierre C, Bhaumik P, Nieminen J. Galectins in innate immunity: dual functions of host soluble beta-galactoside-binding lectins as damage-associated molecular patterns (DAMPs) and as receptors for pathogen-associated molecular patterns (PAMPs). *Immunol Rev*. 2009;230:172–187.
43. Garin MI, Chu CC, Golshayan D, Cernuda-Morollon E, Wait R, Lechler RI. Galectin-1: a key effector of regulation mediated by CD4+CD25+ T cells. *Blood*. 2007;109:2058–2065.
44. Rabinovich GA, Gruppi A. Galectins as immunoregulators during infectious processes: from microbial invasion to the resolution of the disease. *Parasite Immunol*. 2005;27:103–114.
45. Reddy PB, Sehrawat S, Suryawanshi A, et al. Influence of galectin-9/Tim-3 interaction on herpes simplex virus-1 latency. *J Immunol*. 2011;187:5745–5755.
46. Shimmura-Tomita M, Wang M, Taniguchi H, Akiba H, Yagita H, Hori J. Galectin-9-mediated protection from allo-specific T cells as a mechanism of immune privilege of corneal allografts. *PloS One*. 2013;8:e63620.
47. Matsumoto R, Matsumoto H, Seki M, et al. Human ecalectin, a variant of human galectin-9, is a novel eosinophil chemoattractant produced by T lymphocytes. *J Biol Chem*. 1998;273:16976–16984.
48. Kashio Y, Nakamura K, Abedin MJ, et al. Galectin-9 induces apoptosis through the calcium-calpain-caspase-1 pathway. *J Immunol*. 2003;170:3631–3636.
49. Croci DO, Cerliani JP, Dalotto-Moreno T, et al. Glycosylation-dependent lectin-receptor interactions preserve angiogenesis in anti-VEGF refractory tumors. *Cell*. 2014;156:744–758.
50. Hsieh SH, Ying NW, Wu MH, et al. Galectin-1, a novel ligand of neuropilin-1, activates VEGFR-2 signaling and modulates the migration of vascular endothelial cells. *Oncogene*. 2008;27:3746–3753.
51. Markowska AI, Jefferies KC, Panjwani N. Galectin-3 protein modulates cell surface expression and activation of vascular endothelial growth factor receptor 2 in human endothelial cells. *J Biol Chem*. 2011;286:29913–29921.
52. Etulain J, Negrotto S, Tribulatti MV, et al. Control of angiogenesis by galectins involves the release of platelet-derived proangiogenic factors. *PloS One*. 2014;9:e96402.
53. Henderson NC, Mackinnon AC, Farnworth SL, et al. Galectin-3 regulates myofibroblast activation and hepatic fibrosis. *Proc Natl Acad Sci U S A*. 2006;103:5060–5065.
54. Henderson NC, Mackinnon AC, Farnworth SL, et al. Galectin-3 expression and secretion links macrophages to the promotion of renal fibrosis. *Am J Pathol*. 2008;172:288–298.
55. Mackinnon AC, Gibbons MA, Farnworth SL, et al. Regulation of transforming growth factor-beta1-driven lung fibrosis by galectin-3. *Am J Respir Crit Care Med*. 2012;185:537–546.
56. Calvier L, Miana M, Reboul P, et al. Galectin-3 mediates aldosterone-induced vascular fibrosis. *Arterioscler Thromb Vasc Biol*. 2013;33:67–75.
57. Wang YG, Kim SJ, Baek JH, Lee HW, Jeong SY, Chun KH. Galectin-3 increases the motility of mouse melanoma cells by regulating matrix metalloproteinase-1 expression. *Exp Mol Med*. 2012;44:387–393.
58. Kim SJ, Shin JY, Lee KD, et al. Galectin-3 facilitates cell motility in gastric cancer by up-regulating protease-activated receptor-1 (PAR-1) and matrix metalloproteinase-1 (MMP-1). *PloS One*. 2011;6:e25103.
59. Park JE, Chang WY, Cho M. Induction of matrix metalloproteinase-9 by galectin-7 through p38 MAPK signaling in HeLa human cervical epithelial adenocarcinoma cells. *Oncology Rep*. 2009;22:1373–1379.
60. Wu MH, Hong TM, Cheng HW, et al. Galectin-1-mediated tumor invasion and metastasis, up-regulated matrix metalloproteinase expression, and reorganized actin cytoskeletons. *Mol Cancer Res*. 2009;7:311–318.
61. Demers M, Magnaldo T, St-Pierre Y. A novel function for galectin-7: promoting tumorigenesis by up-regulating MMP-9 gene expression. *Cancer Res*. 2005;65:5205–5210.
62. Nishi N, Shoji H, Seki M, et al. Galectin-8 modulates neutrophil function via interaction with integrin alphaM. *Glycobiology*. 2003;13:755–763.

Investigative Ophthalmology & Visual Science